21PM2B-04

Characteristics of Localized Circularly Polarized Light for All-Optical Magnetic Recording

-Field Distribution inside Particulate Media by Changing Antenna Position-

Shinichiro Ohnuki [#1], Tsukasa Kato [#], Yuta Takano [#], Yoshito Ashizawa [#], Katsuji Nakagawa [#]

[#] *College of Science and Technology, Nihon University*
Tokyo, Japan

[1] ohnuki.shinichiro@nihon-u.ac.jp

***Abstract*—All-optical magnetic recording with localized circularly polarized light has been proposed for high density and high speed magnetic recording. In this report, we discuss the Stokes parameters and the figure of merit inside recording media when the plasmonic antenna is moved for simulating recording process.**

I. INTRODUCTION

All-optical magnetic recording with circularly polarized light has been proposed for ultra-high speed recording [1]–[3]. However, the recording density is not high enough in comparison with the conventional magnetic recording because it is difficult to localize the circularly polarized light. Therefore, we designed plasmonic cross antennas to generate the localized circularly polarized light inside bit-patterned media for high density magnetic recording [4]. In this report, we discuss the total intensity enhancement, the degree of circular polarization, and the figure of merit [5] inside the recording media when the plasmonic antenna is moved to simulate recording process.

II. COMPUTATIONAL METHOD AND MODEL

To compute the electromagnetic fields of the dispersive medium, we apply the finite-difference time-domain (FDTD) method with the auxiliary differential equation (ADE) method [6], [7]. In this method, we calculate the electromagnetic fields by using the following equations, which are obtained by coupling the Maxwell equations with the motion equation of an electron expressed by the current and polarization:

$$\mathbf{H}^{n+\frac{1}{2}} = \mathbf{H}^{n-\frac{1}{2}} - \frac{\Delta t}{\mu_0}\left(\nabla \times \mathbf{E}^n\right), \tag{1}$$

$$\mathbf{E}^{n+1} = C_1\mathbf{E}^n + C_2\left[\nabla \times \mathbf{H}^{n+\frac{1}{2}} - \frac{1}{2}\sum_{l=0}^{K}\left\{(1+\alpha_l)\mathbf{J}_l^n - \gamma_l\mathbf{P}_l^n\right\}\right], \tag{2}$$

$$\mathbf{J}_l^{n+1} = \alpha_l\mathbf{J}_l^n + \beta_l\left(\mathbf{E}^{n+1} + \mathbf{E}^n\right) - \gamma_l\mathbf{P}_l^n, \tag{3}$$

$$\mathbf{P}_l^{n+1} = \mathbf{P}_l^n + \frac{\Delta t}{2}\left(\mathbf{J}_l^{n+1} + \mathbf{J}_l^n\right). \tag{4}$$

The three dimensional mesh size 1.0×1.0×1.0 nm^3 and the time increment 1.9×10^{-18} s are selected. The computational domain is surrounded by the convolutional PML (CPML).

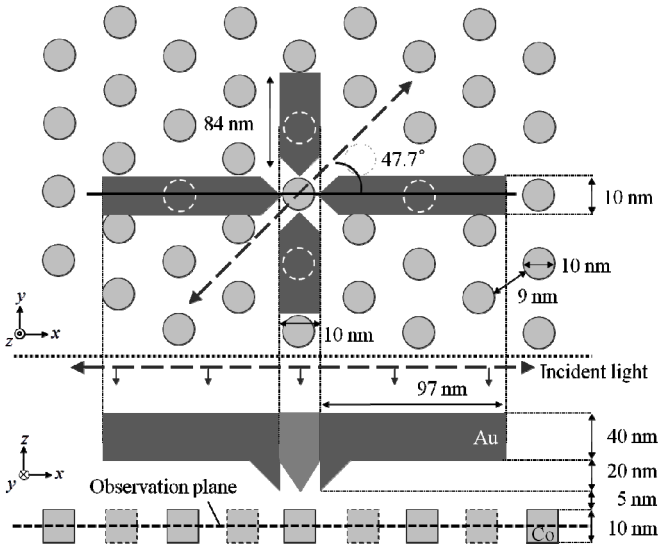

Fig. 1. All-optical magnetic recording system using a plasmonic antenna with bit-patterned media

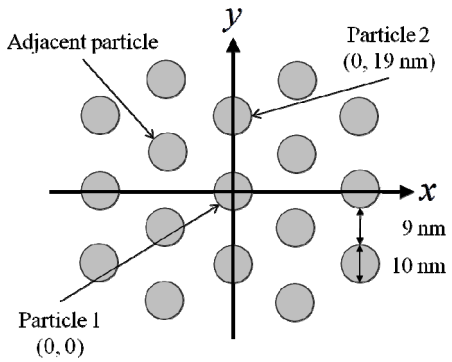

Fig. 2. Arrangement of particles.

Figure 1 shows the plasmonic cross antenna model with the bit-patterned media. These parameters of the antenna and the recording media, whose materials are gold and cobalt, are selected for realizing 2 Tbit/inch^2 recording density. The incident light is a plane wave to propagate toward the negative *z*-axis. The amplitude of the electric field is 1.0 V/m and the wavelength is 780 nm. The observation plane is at the middle of the recording media on the *x*-*y* plane. The angle of the

electric field components of the incident light on the *x*-*y* plane are selected as 47.7 deg to match the value of the electric field components of the *x* and *y* directions.

Figure 2 shows the arrangement of the particles. The plasmonic antenna is moved from the particle 1 to the particle 2 along the *y*-axis for simulating recording process. The particles 1 and 2 are located at the origin and at the positive 19 nm to the *y* direction, respectively. The adjacent particles are the nearest of all particles to the particles 1 and 2.

III. Numerical Results

We investigate the Stokes parameters to discuss the total intensity enhancement *I*, the degree of circular polarization *C'*, and the figure of merit *F* as follows:

$$I = \left\langle E_x^2(t) \right\rangle + \left\langle E_y^2(t) \right\rangle + \left\langle E_z^2(t) \right\rangle, \tag{5}$$

$$C' = \frac{2\left\langle E_x(t) E_y(t) \sin\left(\delta_x - \delta_y\right) \right\rangle}{\left\langle E_x^2(t) \right\rangle + \left\langle E_y^2(t) \right\rangle + \left\langle E_z^2(t) \right\rangle}, \tag{6}$$

$$F = C' \times I . \tag{7}$$

Figure 3 shows the field distributions of the total intensity enhancement *I* at the middle of the bit-patterned media on the *x*-*y* plane in the recording process. The intensity *I* of particle 1 is the highest of all particles as shown in Figure 3(a). Figure 4 shows the intensity *I* of each particle when the position of the plasmonic antenna is changed from the particles 1 to 2. The intensity *I* of the particles 1 and 2 become higher than those of the adjacent particles despite of the antenna position.

Figure 5 shows the field distributions of the degree of circular polarization *C'* at the middle of the bit-patterned media on the *x*-*y* plane. Circularly polarized light is generated by using the plasmonic antenna only inside the particle 1 as shown in Figure 5(a). If the plasmonic antenna is located between the particle 1 and 2, the circularly polarized light is not generated inside any particles as shown in Figure 5(b). Figure 6 shows the circularity *C'* of each particle when the plasmonic antenna position is changed from particles 1 to 2. We can confirm that the highest value of the circularity *C'* can be obtained when the antenna is located just above the particles 1 and 2.

Figure 7 shows the field distributions of the figure of merit *F* at the middle of the bit-patterned media on the *x*-*y* plane. The *F* of the particle 1 becomes the highest of all particles as shown in Figure 7(a). Figure 8 shows the *F* of each particle when the plasmonic antenna position is changed from the particles 1 to 2. When the *F* of the particle 1 is higher, the *F* of particle 2 becomes lower for varying the antenna position. Moreover, the adjacent particle keeps the lowest value of the *F* in this recording process.

IV. Conclusions

We design the plasmonic cross antenna with the bit-patterned media for all-optical recording. The total intensity enhancement, the degree of circular polarization, and the figure of merit are discussed for changing the antenna position. The circularly polarized light is generated only inside the purposed particles. Moreover, the figure of merit shows when

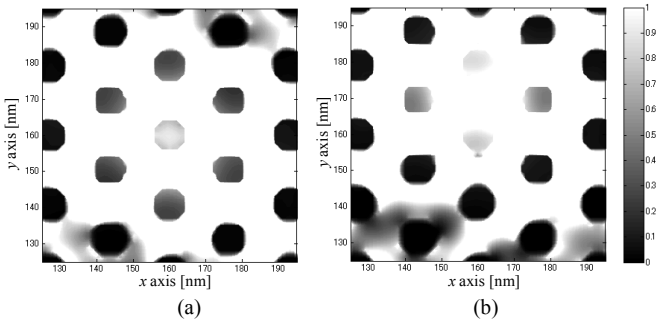

Fig. 3. Field distributions of the total intensity enhancement *I* at the middle of the bit-patterned media on the *x*-*y* plane in the recording process. (a) The plasmonic antenna is located on the particle 1 (*y* = 0 nm), and (b) located between the particles 1 and 2 (*y* = +10 nm).

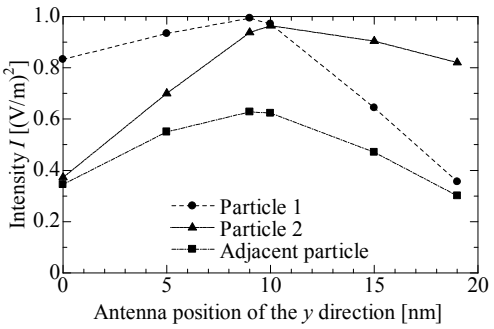

Fig. 4. Total intensity enhancement *I* of each particle when the plasmonic antenna position is changed from the particle 1 (*y* = 0 nm) to the particle 2 (*y* = +19 nm).

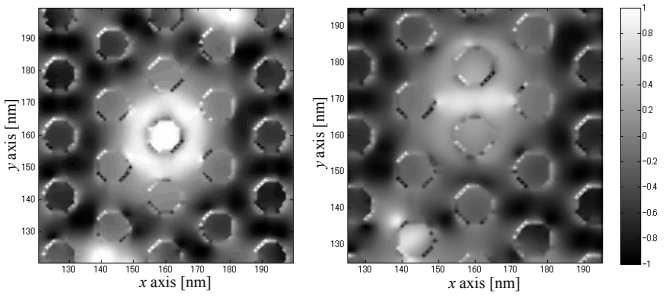

Fig. 5. Field distributions of the degree of circular polarization *C'* at the middle of the bit-patterned media on the *x*-*y* plane in the recording process. (a) The plasmonic antenna is located on the particle 1 (*y* = 0 nm), and (b) located between the particle 1 and 2 (*y* = +10 nm).

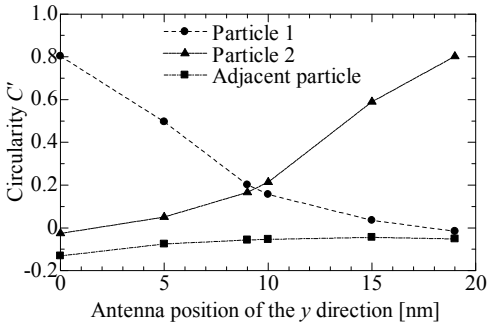

Fig. 6. Degree of circular polarization *C'* of each particle when the plasmonic antenna position is changed from the particle 1 (*y* = 0 nm) to the particle 2 (*y* = +19 nm).

the antenna position is changed from the particle 1 to the particle 2.

ACKNOWLEDGMENTS

This work is party supported by Grant-in-Aid for Scientific Research (C) (22560349), CASIO Science Promotion Foundation, and Nihon University Strategic Projects for Academic Research.

REFERENCES

[1] C. D. Stanciu, F. Hansteen, A. V. Kimel, A. Kirilyuk, A. Tsukamoto, A. Itoh, and Th. Rasing, "All-Optical Magnetic Recording with Circularly Polarized light," *Phys. Rev. Lett.*, Vol. 99, pp. 047601-1–047601-4 , Jul. 2007.

[2] K. Nakagawa, J. Kim, and A. Itoh, "Near-field optically assisted hybrid head for self-aligned Plasmon spot with magnetic field," *J. Appl. Phys*., Vol. 99, pp. 08F902-1–08F902-3, Apr. 2006.

[3] K. Nakagawa, Y. Ashizawa, S. Ohnuki, A. Itoh, and A. Tsukamato, "Confined circularly polarized light generated by nano-size aperture for high density all-optical magnetic recording," *J. Appl. Phys.*, Vol. 109, pp. 07B735-1–07B735-3, Apr. 2011.

[4] H. Iwamatsu, T. Kato, S. Ohnuki, Y. Ashizawa, K. Nakagawa, and W. C. Chew, "Analysis of Electromagnetic fields of a Plasmonic Cross Antenna with Bit-Patterned Media," Proc. 2012 IEEE International Symposium on Antennas and Propagation and USNC/URSI Radio Science Meeting, IF22.7, Jul. 2012.

[5] P. Biagioni, J. S. Huang, L. Duò, M. Finazzi, and B.Hecht, "Cross Resonant Optical Antenna," *Phys. Rev. Lett.*, Vol. 102, pp. 256801-1–1256801-4, Jun. 2009.

[6] T. Yamaguchi and T. Hinata, "Optical near-field analysis of spherical metals: Application of the FDTD method combined with the ADE method," *Opt. Express*, Vol. 15, pp. 11481–11491, Sep. 2007.

[7] Rakić, A. D., A. B. Djurišić, J. M. Elazar, and M. L. Majewski, "Optical Properties of Metallic Films for Vertical-Cavity Optoelectronic devices," *Appl. Opt.*, Vol. 37, pp. 5271–5283, Aug. 1998.

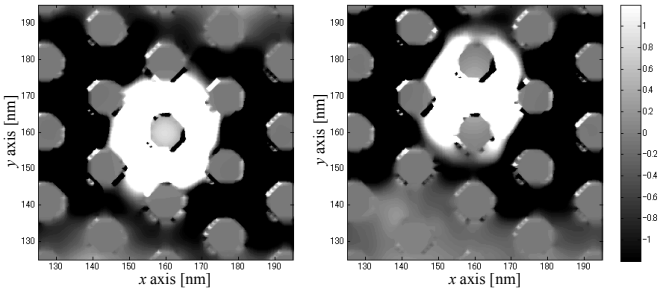

Fig. 7. Field distributions of the figure of merit F at the middle of the bit-patterned media on the x-y plane in the recording process. (a) The plasmonic antenna is located on the particle 1 (y = 0 nm), and (b) located between the particle 1 and 2 (y = +10 nm).

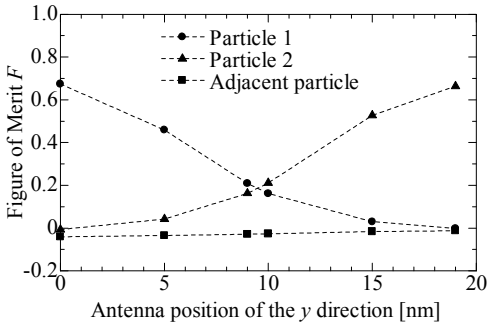

Fig. 8. Figure of merit F of each particle when the plasmonic antenna position is changed from the particle 1 (y = 0 nm) to the particle 2 (y = +19 nm).